

## **COARSE GRID NUMERICAL SIMULATION OF REACTION KINETICS MODEL IN THE GAS HYDRATE RESERVOIRS**

**Amir Shahbazi**

**Department of Chemical & Petroleum Engineering  
University of Calgary  
2500 University Drive NW, Calgary, AB, T2N 1N4  
CANADA**

**Mehran Pooladi-Darvish\***

**Department of Chemical and Petroleum Engineering  
University of Calgary  
2500 University Drive NW, Calgary, AB, T2N 1N4, and  
Fekete Associates Inc.  
Suite 2000, 540 – 5<sup>th</sup> Ave SW  
Calgary, AB, T2P 0M2  
CANADA**

**Hassan Hassanzadeh**

**R&D Directorate  
Iranian National Oil Company (NIOC)  
Tehran  
Iran**

### **ABSTRACT**

A number of simulation studies of hydrate decomposition in porous media have shown hydrate decomposition zone could be narrow, especially when permeability at initial hydrate saturation is low. Field scale simulation of gas production from hydrate reservoirs with (fine) grid blocks that allow accurate modeling of the decomposition region becomes impractical.

This paper proposes a methodology for the use of coarse grid blocks for the simulation of hydrate decomposition without loss of accuracy. This study focuses on the modeling of an energy self sustaining gas production process from hydrate reservoir known as depressurization technique. In this process the pressure reduction diffuses within the hydrate layer resulting in the decomposition of hydrate structures and gas generation. A 1-D mathematical model is introduced which incorporates energy balance, fluid flow and kinetics of hydrate decomposition. Numerical results are shown to demonstrate the lack of accuracy of this solution when coarse grid blocks are used. This study uses Taylor series and determines additional terms and a correction parameter ( $\alpha$ ), which when are incorporated in the coarse-grid model improves its accuracy. It is shown that a single value of correction parameter ( $\alpha$ ) is sufficient to improve the accuracy of all variables (pressure, temperature and hydrate saturation), and for all times. A relation is obtained between the correction parameter and the coarse-grid size. The success of methodology in improving the accuracy of modeling with coarse grid cells and matching the results of a solution with a highly refined grid has been demonstrated for two systems with various properties.

*Keywords:* hydrate decomposition, reaction kinetics, numerical reaction upscaling

---

\* Corresponding author: Phone: +1 403 213 4429 Fax +1 403 284 4852 E-mail: pooladi@ucalgary.ca

## INTRODUCTION

Hydrate particles are made up of natural gas molecules trapped in water molecule structures, and are considered as a potential resource for clean energy. Enormous quantities of methane gas exist in the form of hydrate in the permafrost and offshore environments. Large resources of hydrate have been explored worldwide including the North West Territories of Canada, Siberia, Alaska and Japan. In the last two decades much interest and research has been devoted towards the mathematical modeling of gas production from hydrate reservoirs. The main mechanisms involved in the process of hydrate decomposition and gas production are thermodynamic and kinetics of decomposition, heat transfer from the surrounding area or from an external source of heat to the decomposition zone as well as gas-water flow inside the reservoir.

Three general techniques have been suggested to recover gas from hydrate reservoirs which are all based on breaking the stability conditions of hydrate leading to generation of gas; Depressurization, Thermal Stimulation and Inhibitor Injection. While depressurization does not require an external source of energy and is based on propagation of pressure drop from the wellbore to the hydrate decomposition zone, the thermal stimulation technique needs an external source of energy, not unlike those applied in the thermal recovery of heavy oils. Efficiency and economics of these techniques is the subject of numerous investigations.

The first attempts to model hydrate formation and decomposition go back to the works done in the first decades of 1900's which aimed at preventing hydrate formation in the gas transportation pipes. Exploration of hydrate reservoirs and their potential as a new resource for energy has resulted in more research activities in the last two decades.

The existing analytical models (Selim and Sloan [1] in 1985, Selim and Sloan [2] in 1990, Tsytkin [3] in 2000, Hong et al [4] in 2002, and Gerami and Pooladi-Darvish [5,6] in 2006) have been used as a tool for mechanistic studies and understanding of the behavior of the decomposition process. However the limitations and assumptions involved in the analytical models limits their application.

Numerical models (Holder and Angert [7] in 1982, Burshears et al [8] in 1986, Yousif et al [9] in 1991, Moridis [10] in 2002, Hong and Pooladi-Darvish [11] in 2003, Moridis et al [12] in 2005, and Sun and Mohanty [13] in 2005) are based on a more general form of the mathematical model of the process and can be easily extended to include real-life conditions such as heterogeneity and variable operating conditions.

A number of these simulation studies have indicated that hydrate decomposition occurs over a relatively narrow zone, leading to very sharp gradients. In the depressurization technique this occurs especially when the effective permeability of the hydrate-bearing porous medium is low. (At the limit, when permeability approaches zero, decomposition occurs on a sharp interface.) The narrow decomposition zone requires small grid blocks for accuracy of the numerical solution. Despite the small length scale of the decomposition front, the length scale of the temperature and pressure fronts are significantly larger [14]. Large-scale simulation of such coupled processes, with multi-scale phenomena which require small grid-blocks is computationally expensive.

In this paper, we provide a methodology for accurate numerical solution of the hydrate decomposition problem using coarse grid-blocks. The paper is organized as follows. First, the mathematical model of gas hydrate decomposition used in this study is presented. Next, grid dependency of the solution is demonstrated through a set of numerical simulations. The methodology for adding corrections to the coarse grid model to improve its accuracy, which is based on the Taylor's series expansion of the coarse grid solution, is then presented. Finally the application of this methodology for improving accuracy of coarse-grid simulation of hydrate decomposition is presented. The limitations of the method are finally presented.

## MATHEMATICAL MODEL OF GAS HYDRATE DECOMPOSITION

The process of gas production from hydrate reservoir involves three major mechanisms; heat transfer by conduction and convection, endothermic reaction that convert hydrate structure to gas and water molecules and flow of products in the reservoir.

We assume a semi infinite 1-D hydrate layer which is initially at equilibrium pressure  $p_i$  corresponding to initial temperature  $T_i$ . At  $t = 0$  the pressure at  $x = 0$  is reduce to  $p_0$  which is less than initial pressure  $p_i$ . According to the Kim-Bishnoi [15] model for hydrate decomposition, the difference between gas pressure in the bulk and the three-phase equilibrium pressure<sup>1</sup> at the hydrate temperature provides the driving force for hydrate decomposition. Since the pressure at inlet is less than equilibrium pressure corresponding to the local temperature, the decomposition of hydrate commences and moves into the hydrate layer. The heat of decomposition leads to reduced temperature and results in heat flow from warmer parts of the porous medium towards the decomposition zone. Depending on how fast pressure reduction can diffuse within the porous medium and its competition with heat flow [14], decomposition zone can be narrow or wide. In the following we will present a mathematical model that describes the processes described above. However, we will use a number of assumptions and simplifications that include:

1. The mass transfer caused by molecular diffusion is small.
2. Convective heat transfer is neglected.
3. Conductive heat transfer at the production end is negligible.
4. The phase equilibrium relation is approximated by a straight line.
5. The mobility of the gas is much more than that of the water, such that the pressure gradient in the porous medium is related to flow of water.
6. Capillary pressure is ignored.

<sup>1</sup> The more accurate expression is fugacity which can be defined for any state of material.

## FORMULATION

Here, three differential equations are derived to describe changes in hydrate saturation, and flow of energy and water.

### 1. Hydrate mass balance

Using Kim-Bishnoi [15] Kinetics model, the rate of decomposition of hydrate molecules can be written as:

$$\frac{dm_H}{dt} = -k_d(T)M_H a_{dec} (p_{eq} - p_g) a_{geo} \Delta x \quad (1)$$

where an Arrhenius type relation has been suggested

for the reaction constant [15],  $k_d(T) = k_0 e^{-\frac{E}{RT}}$ ,

$a_{dec}$  is the total surface available for decomposition and is defined as  $a_{dec} = S_H \phi a_{HS}$  and  $a_{HS}$  is total surface of hydrate structure per unit volume.

The mass rate of hydrate decomposition can also be written as:

$$\frac{dm_H}{dt} = V_b \rho_H \phi \frac{dS_H}{dt} \quad (2)$$

Thermodynamic equilibrium relations of hydrates are presented by Sloan [16]. Over a small range of temperature change, corresponding to what happens in the depressurization, we use a linear approximation (assumption 4),

$$p_{eq} = b_1 + b_2 T_{eq} \quad (3)$$

Using this relation, and assuming local temperature equilibrium, equations 1 and 2 may be combined to obtain:

$$\frac{dS_H}{dt} = -\frac{M_H a_{HS} b_2}{\rho_H} k_0 e^{-\frac{E}{RT}} S_H (T - T_{eq}) \quad (4)$$

### 2. Energy balance:

The energy required for the reaction is provided by heat conduction from deep within the hydrate layer and sensible heat of the porous medium and its constituents,

$$\frac{\partial^2 T}{\partial x^2} - \frac{M_H \phi a_{HS} b_2 \Delta H}{k} k_o e^{-\frac{E}{RT}} S_H (T - T_{eq}) = \frac{1}{\alpha} \frac{\partial T}{\partial t} \quad (5)$$

### 3. Water mass balance:

The pressure equation for water may be obtained by combining Darcy's law and the continuity equation accounting for the water generated due to the decomposition of hydrate:

$$\frac{\partial}{\partial x} \left( \rho_w \frac{K(S_w) k_{rw}}{\mu_w} \frac{\partial p_w}{\partial x} \right) + q_w = \frac{\partial}{\partial t} (\phi \rho_w S_w) \quad (6)$$

The mass rate of water generation per unit bulk volume is calculated based on hydration number defined as the ratio of water molecules to gas molecules within a hydrate structure. ( $N_H = 5.75$ )

$$q_w = N_H \frac{M_w}{M_g} q_g, \quad q_g = -\frac{M_g}{M_H} q_H, \quad q_H = \frac{d}{dt} (\phi \rho_H S_H)$$

$$\text{and } q_w = -N_H \frac{M_w}{M_H} \frac{\partial}{\partial t} (\phi \rho_H S_H)$$

where  $M_H$ ,  $M_g$  and  $M_w$  are molecular weights of hydrate, gas and water. Assuming that gas mobility is infinite per assumption 5 (i.e. gas leaves the porous media immediately after generation), equation (6) may be written as:

$$\frac{\partial}{\partial x} \left( \frac{K(S_H) k_{rw}}{\mu_w} \frac{\partial p_w}{\partial x} \right) = \quad (7)$$

$$\phi \left( N_H \frac{\rho_H}{\rho_w} \frac{M_w}{M_H} - C \right) \frac{\partial S_H}{\partial t}$$

Where  $C$  is a constant.

Ignoring capillary pressure,  $p_g = p_w = p$ .

Masuda et al [17] suggested that the permeability of the hydrate-bearing porous medium is significantly reduced as the hydrate saturation is increased. They proposed a correlation given as:

$$K(S_H) = K_0 (1 - S_H)^m$$

where  $K$  is permeability in the presence of hydrate and  $K_0$  is intrinsic absolute permeability (without hydrate) [17,18]. They suggested values between 2 to 15 for the index  $m$ . We use this relation to evaluate the effective permeability of the porous medium to water in the presence of solid hydrate.

## EQUATIONS IN THE DIMENSIONLESS FORM

The following dimensionless variables have been introduced:

$$\xi = \frac{x}{l_{ref}} \quad \tau = \frac{\alpha t}{l_{ref}^2} \quad \theta = \frac{T - T_b}{T_i - T_b}$$

$$\Omega = \frac{p - p_0}{p_i - p_0} \quad c = \frac{S_H}{S_{Hi}}$$

where  $l_{ref} = \sqrt{\frac{\alpha}{\kappa}}$ ,  $\kappa = \frac{\eta R T_b^2}{E} e^{-\frac{E}{RT_b}}$  ( $\frac{1}{Sec}$ ) and

$$\eta = \frac{k_o M_H a_{HS} b_2}{\rho_H} \left( \frac{1}{K \cdot Sec} \right)$$

Here  $T_b$  is reference temperature which is defined as an adiabatic temperature:

$$\rho C_p (T_i - T_b) = \phi \rho_H S_{Hi} \Delta H$$

Using the above dimensionless variables the equations of mass, heat and reaction may be written as:

$$\frac{\partial c}{\partial \tau} = -Z_e c e^{\varepsilon Z_e \theta + 1} (\theta - \theta_{eq}) \quad (9a)$$

$$\frac{\partial^2 \theta}{\partial \xi^2} - Z_e c e^{\varepsilon Z_e \theta + 1} (\theta - \theta_{eq}) = \frac{\partial \theta}{\partial \tau} \quad (9b)$$

$$\frac{\partial}{\partial \xi} \left( (1 - S_{Hi} c)^m \frac{\partial \Omega}{\partial \xi} \right) = \pi \frac{\partial c}{\partial \tau} \quad (9c)$$

$$\theta_{eq} = a_1 + a_2 \Omega \quad (9d)$$

$$\text{Where: } Z_e = \frac{\rho_H \phi \Delta H S_{Hi}}{\rho C_p R T_b^2} = \frac{E(T_i - T_b)}{R T_b^2},$$

$$\varepsilon = \frac{R T_b}{E}, \quad \pi = \frac{\phi \mu_w S_{Hi} \alpha (N_H \frac{\rho_H}{\rho_w} \frac{M_w}{M_H} - C)}{K_0 (P_i - P_0)},$$

$$a_1 = \frac{p_0 - (b_1 + b_2 T_b)}{b_2 (T_i - T_b)}, \quad \text{and } a_2 = \frac{(p_i - p_0)}{b_2 (T_i - T_b)}$$

Zeldovich number  $Z_e$  is a dimensionless activation energy [19] defined as the ratio of the diffusion temperature scale  $T_i - T_b$  to the reaction temperature

$$\text{scale [20] } \frac{R T_b^2}{E}.$$

Typical values of  $E$ ,  $R$  and  $T_b$  show that  $\varepsilon$  is a very small value ( $\frac{RT_b}{E} = \frac{275}{9750} \approx 0$ ), resulting in

$e^{\frac{Z_e \theta}{\varepsilon Z_e \theta + 1}} = e^{Z_e \theta}$ . Rewriting the equations:

$$\frac{\partial c}{\partial \tau} = -Z_e c e^{Z_e \theta} (\theta - \theta_{eq}) \quad (10a)$$

$$\frac{\partial^2 \theta}{\partial \xi^2} - Z_e c e^{Z_e \theta} (\theta - \theta_{eq}) = \frac{\partial \theta}{\partial \tau} \quad (10b)$$

$$\frac{\partial}{\partial \xi} \left( (1 - S_{Hi} c)^m \frac{\partial \Omega}{\partial \xi} \right) = \pi \frac{\partial c}{\partial \tau} \quad (10c)$$

$$\theta_{eq} = a_1 + a_2 \Omega \quad (10d)$$

For the problem described earlier, the initial and boundary conditions may be expressed as,

$$\theta = 1 \quad \tau = 0, \quad 0 < \xi < \infty \quad (10e)$$

$$c = 1 \quad \tau = 0, \quad 0 < \xi < \infty \quad (10f)$$

$$\Omega = 1 \quad \tau = 0, \quad 0 < \xi < \infty \quad (10g)$$

$$\frac{\partial \theta}{\partial \xi} = 0 \quad \tau = 0^+, \quad \xi = 0 \quad (10h)$$

$$\theta = 1 \quad \tau = 0^+, \quad \xi \rightarrow \infty \quad (10i)$$

$$\Omega = 0 \quad \tau = 0^+, \quad \xi = 0 \quad (10j)$$

$$\Omega = 1 \quad \tau = 0^+, \quad \xi \rightarrow \infty \quad (10k)$$

## NUMERICAL RESULTS AND GRID DEPENDENCY OF THE SOLUTION

Equations 10a to 10k have been solved numerically using finite difference scheme in fully implicit form. A base case run using 500 spatial grid blocks has been conducted as the reference solution. Simulation of higher number of grid blocks proved that simulation with 500 grid blocks gives accurate results. Table 1 lists parameters used in these simulations. Based on the values in Table 1 the dimensionless groups  $Z_e, \pi$ , bulk physical properties of formation, adiabatic temperature and

dimensionless linear phase equilibrium constants were calculated and listed in Table 2.

Initial hydrate saturation $S_{Hi}$	0.35
Porosity $\phi$	0.2
Hydrate density $\rho_H$	919.7 $kg/m^3$
Rock density $\rho_R$	2650 $kg/m^3$
Water density $\rho_w$	1000 $kg/m^3$
Latent heat of reaction $\Delta H$	477 $kJ/kg$
Initial temperature $T_i$	288 $^\circ K$
Heat capacity of water $C_{pw}$	4.18 $kJ/^\circ Kkg$
Heat capacity of hydrate $C_{pH}$	1.6 $kJ/Kkg$
Heat capacity of rock $C_{pR}$	0.8 $kJ/Kkg$
Thermal conductivity of water $k_w$	0.6 $kw/Km$
Thermal conductivity of hydrate $k_H$	0.393 $kw/Km$
Thermal conductivity of rock $k_R$	1.5 $kw/Km$
Activation Energy $E/R$	9750 $1/K$
Linear phase equilibrium constant $b_1$	-170.71 $MPa$
Linear phase equilibrium constant $b_2$	0.6327 $MPa/K$
Initial pressure $P_i$	11.51 $MPa$
Pressure at the inlet $P_0$	2.213 $MPa$
Hydration number $N_H$	5.75
Hydrate Molecular weight $M_H$	119.543 $kg/kmole$
Water Molecular weight $M_w$	18.02 $kg/kmole$
Water viscosity $\mu_w$	0.001 $Pa.S$
Permeability power index $m$	15
Absolute permeability $K_0$	1.00E-15 $m^2$

**Table 1**

Dimensionless pressure, hydrate saturation and temperature profiles for the base case and two coarse solutions using 100 and 50 grid blocks are shown in Figure 1.

$\rho \cdot C_p$	2342.4 $kJ / Km^3$
$k$	1.306 $kW / Km$
$\alpha$	5.57E-07 $m^2 / S$
$T_b$	274.89 $K$
$Z_e$	1.691
$a_1$	-0.1206
$a_2$	1.1206
$\pi$	0.002507

**Table 2**

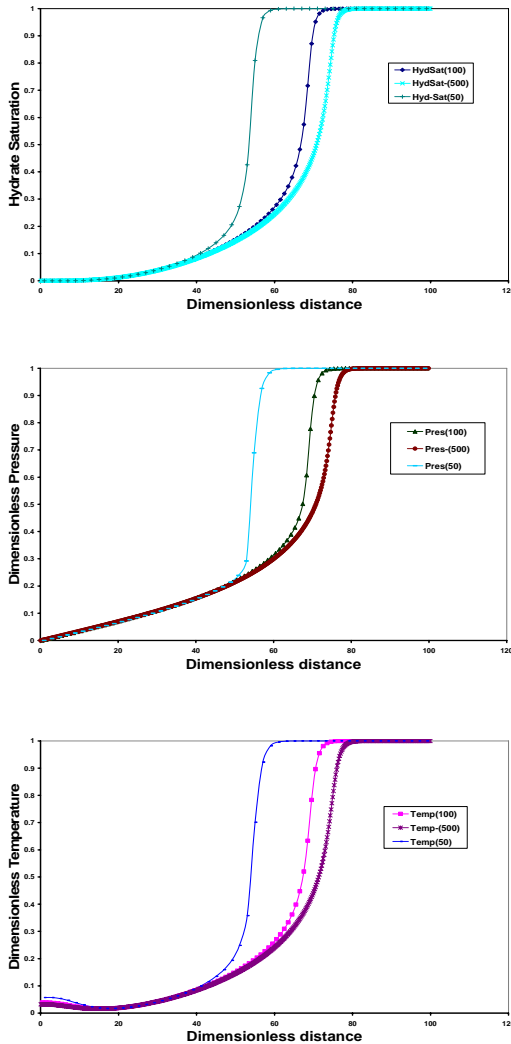


**Figure 1:** Dimensionless hydrate saturation, pressure and temperature for the fine and coarse grid simulations at dimensionless time = 30

The results shown in Figure 1 indicate that deviations from reference solution are severe, and that the coarse grid solution misses the reaction front. This would lead to a smaller decomposed zone and slower rate of gas generation. Simulation studies of hydrates in porous media reported by Zatsepina et al. [14] showed a similar response, where the coarse grid solutions indicated a lower rate of gas generation for a hydrate layer sandwiched between two shale layers.

The difference between the coarse and fine-grid solution is also shown in Figure 2, where the dimensionless rate of hydrate decomposition is shown. Similar deviations were observed in different times and with different sets of parameters.

$$\text{Reaction Rate} = -Z_e c e^{Z_e \theta} (\theta - \theta_{eq})$$

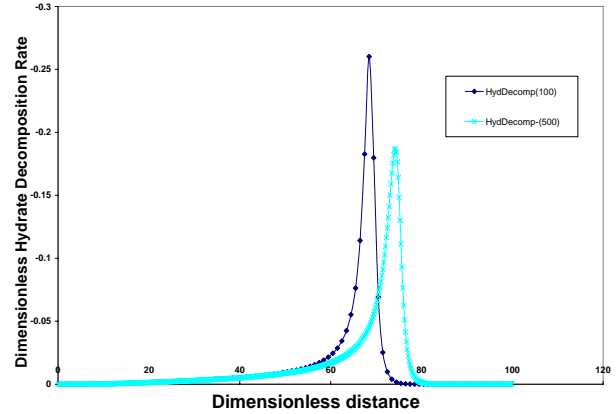


**Figure 2:** Dimensionless rate of reaction from the coarse and fine-grid solutions at dimensionless time = 30.

In the following we will develop a methodology for improving the accuracy of the coarse-grid model.

### APPLYING TAYLOR SERIES TO IMPROVE THE COARSE-GRID SOLUTION

To improve the accuracy of the coarse-grid model, we intend to develop a relationship for an “equivalent” reaction-rate, which when incorporated in the coarse-grid model improves its accuracy. We use the following definition to represent the value of a property over a coarse grid:

$$\bar{\psi} = \frac{1}{V} \int_V \psi dv \quad (11)$$

where  $\psi$  can be temperature, pressure or hydrate saturation and  $V$  represents a coarse grid in the numerical model.

The fine-grid model was given by equations 10 as:

$$\frac{\partial c}{\partial \tau} = -Z_e \mathfrak{R} \quad (12a)$$

$$\frac{\partial \theta}{\partial \tau} = \frac{\partial^2 \theta}{\partial \xi^2} - Z_e \mathfrak{R} \quad (12b)$$

$$\frac{\partial}{\partial \xi} \left( (1 - S_{Hi} c)^m \frac{\partial \Omega}{\partial \xi} \right) = \pi \frac{\partial c}{\partial \tau} \quad (12c)$$

where  $\mathfrak{R} = ce^{Z_e \theta} (\theta - \theta_{eq})$  is the fine-grid reaction rate.

The coarse-grid numerical model [21] of equations 12 using definition of average variable (equation 11) can be written as:

$$\frac{\partial \bar{c}}{\partial \tau} = -Z_e \bar{\mathfrak{R}} \quad (13a)$$

$$\frac{\partial \bar{\theta}}{\partial \tau} = \frac{\partial^2 \bar{\theta}}{\partial \xi^2} - Z_e \bar{\mathfrak{R}} \quad (13b)$$

$$\frac{\partial}{\partial \xi} \left( (1 - S_{Hi} \bar{c})^m \frac{\partial \bar{\Omega}}{\partial \xi} \right) = \pi \frac{\partial \bar{c}}{\partial \tau} \quad (13c)$$

Where coarse-grid reaction rate  $\bar{\mathfrak{R}}$  is defined as:

$$\bar{\mathfrak{R}} = \frac{1}{V} \int_V ce^{Z_e \theta} (\theta - \theta_{eq}) dv = \overline{ce^{Z_e \theta} (\theta - \theta_{eq})} \quad (14)$$

The reaction rate  $\mathfrak{R}$  can be approximated by a Taylor series expansion around the coarse grid temperature, concentration and pressure. For this purpose, we define new variables  $c' = c - \bar{c}$ ,  $\Omega' = \Omega - \bar{\Omega}$  and  $\theta' = \theta - \bar{\theta}$ , which are the hydrate saturation, pressure and temperature deviations from the fine-grid solution, respectively. Thus,

$$\begin{aligned} \mathfrak{R}(\theta, \Omega, c) &= \mathfrak{R}(\bar{\theta}, \bar{\Omega}, \bar{c}) \\ &+ \left[ \theta' \frac{\partial \mathfrak{R}}{\partial \theta} + \Omega' \frac{\partial \mathfrak{R}}{\partial \Omega} + c' \frac{\partial \mathfrak{R}}{\partial c} \right] + \\ &\frac{1}{2} \left[ \theta'^2 \frac{\partial^2 \mathfrak{R}}{\partial \theta^2} + \Omega'^2 \frac{\partial^2 \mathfrak{R}}{\partial \Omega^2} + c'^2 \frac{\partial^2 \mathfrak{R}}{\partial c^2} + \right. \\ &\left. 2\theta'c' \frac{\partial^2 \mathfrak{R}}{\partial \theta \partial c} + 2\Omega'c' \frac{\partial^2 \mathfrak{R}}{\partial \Omega \partial c} + 2\theta'\Omega' \frac{\partial^2 \mathfrak{R}}{\partial \theta \partial \Omega} \right] \end{aligned} \quad (15)$$

If one applies the averaging operator to the reaction rate, the averaged reaction rate can be expressed by:

$$\begin{aligned} \bar{\mathfrak{R}}(\theta, \Omega, c) &= \mathfrak{R}(\bar{\theta}, \bar{\Omega}, \bar{c}) + \\ &\frac{1}{2} \left[ \overline{\theta'^2 \frac{\partial^2 \mathfrak{R}}{\partial \theta^2}} + \overline{\Omega'^2 \frac{\partial^2 \mathfrak{R}}{\partial \Omega^2}} + \overline{c'^2 \frac{\partial^2 \mathfrak{R}}{\partial c^2}} \right. \\ &\left. + 2\overline{\theta'c' \frac{\partial^2 \mathfrak{R}}{\partial \theta \partial c}} + 2\overline{\Omega'c' \frac{\partial^2 \mathfrak{R}}{\partial \Omega \partial c}} + 2\overline{\theta'\Omega' \frac{\partial^2 \mathfrak{R}}{\partial \theta \partial \Omega}} \right] \end{aligned} \quad (16)$$

The terms with first derivatives may be ignored [21]. The other terms account for the information that is usually lost in a coarse grid numerical solution.

Using the definition of the reaction term,  $\mathfrak{R} = ce^{Z_e \theta} (\theta - \theta_{eq})$  one can obtain the derivative of reaction with respect to various variables as required in Equation (16) to obtain:

$$\frac{\partial \bar{c}}{\partial \tau} = -Z_e \bar{\mathfrak{R}}(\bar{\theta}, \bar{\Omega}, \bar{c}) -$$

$$\frac{Z_e}{2} \left[ \overline{\theta'^2 \frac{\partial^2 \mathfrak{R}}{\partial \theta^2}} + 2\overline{\theta'c' \frac{\partial^2 \mathfrak{R}}{\partial \theta \partial c}} \right. \\ \left. + 2\overline{\Omega'c' \frac{\partial^2 \mathfrak{R}}{\partial \Omega \partial c}} + 2\overline{\theta'\Omega' \frac{\partial^2 \mathfrak{R}}{\partial \theta \partial \Omega}} \right] \quad (17a)$$

$$\frac{\partial \bar{\theta}}{\partial \tau} = \frac{\partial^2 \bar{\theta}}{\partial \xi^2} - Z_e \bar{\mathfrak{R}}(\bar{\theta}, \bar{\Omega}, \bar{c}) -$$

$$\frac{Z_e}{2} \left[ \overline{\theta'^2 \frac{\partial^2 \mathfrak{R}}{\partial \theta^2}} + 2\overline{\theta'c' \frac{\partial^2 \mathfrak{R}}{\partial \theta \partial c}} \right. \\ \left. + 2\overline{\Omega'c' \frac{\partial^2 \mathfrak{R}}{\partial \Omega \partial c}} + 2\overline{\theta'\Omega' \frac{\partial^2 \mathfrak{R}}{\partial \theta \partial \Omega}} \right] \quad (17b)$$

$$\frac{\partial}{\partial \xi} \left( (1 - S_{Hi} \bar{c})^m \frac{\partial \bar{\Omega}}{\partial \xi} \right) = \pi \frac{\partial \bar{c}}{\partial \tau} \quad (17c)$$

The derivatives expressed in Equation (17) need to be evaluated at  $\theta = \bar{\theta}$ ,  $\Omega = \bar{\Omega}$ , and  $c = \bar{c}$ .

The above system of PDE's is a coarse grid representation of the hydrate decomposition process that requires both coarse and the fine-grid solutions. However, the fine-grid solutions represented as deviation terms  $c'$ ,  $\Omega'$  and  $\theta'$  are not available. It is suggested [22,23] that the quantities  $\overline{(\theta')^2}$ ,  $\overline{\theta'\Omega'}$  and  $\overline{\theta'c'}$  may be expressed in a form proportional to  $\frac{\partial\bar{\theta}}{\partial\xi}$ ,  $\left(\frac{\partial\bar{\theta}}{\partial\xi}\right)\left(\frac{\partial\bar{\Omega}}{\partial\xi}\right)$ ,  $\left(\frac{\partial\bar{c}}{\partial\xi}\right)\left(\frac{\partial\bar{\Omega}}{\partial\xi}\right)$  and  $\left(\frac{\partial\bar{\theta}}{\partial\xi}\right)\left(\frac{\partial\bar{c}}{\partial\xi}\right)$ , such that the final coarse-grid model can be presented as a function of coarse-grid solutions only. The common practice in a volume averaging method [22,23,24,25] is to solve the closure problem which is obtained by subtraction of the fine-grid and the coarse-grid equations. Here, due to the complexity arising from the nonlinearity of the problem, subtraction does not lead to (an) equation(s) in terms of the perturbed quantities. However, consistent with the volume averaging method [22,23] an appropriate approximation for the deviation terms is linear proportionality of temperature and concentration deviations with their corresponding gradient. Using this approximation, one may write:

$$\overline{(\theta')^2} = \alpha \left( \frac{\partial\bar{\theta}}{\partial\xi} \right)^2 \quad (18a)$$

$$\overline{c'\theta'} = \alpha \left( \frac{\partial\bar{\theta}}{\partial\xi} \right) \left( \frac{\partial\bar{c}}{\partial\xi} \right) \quad (18b)$$

$$\overline{\Omega'\theta'} = \alpha \left( \frac{\partial\bar{\theta}}{\partial\xi} \right) \left( \frac{\partial\bar{\Omega}}{\partial\xi} \right) \quad (18c)$$

$$\overline{\Omega'c'} = \alpha \left( \frac{\partial\bar{c}}{\partial\xi} \right) \left( \frac{\partial\bar{\Omega}}{\partial\xi} \right) \quad (18d)$$

Substituting Equations (18) in (17), leads to the coarse-grid equations:

$$\begin{aligned} \frac{\partial\bar{c}}{\partial\tau} = & -Z_e \mathfrak{R}(\bar{\theta}, \bar{\Omega}, \bar{c}) \\ & - \alpha Z_e \left[ \frac{1}{2} \left( \frac{\partial\bar{\theta}}{\partial\xi} \right)^2 \frac{\partial^2 \mathfrak{R}}{\partial\theta^2} + \left( \frac{\partial\bar{\theta}}{\partial\xi} \right) \left( \frac{\partial\bar{c}}{\partial\xi} \right) \frac{\partial^2 \mathfrak{R}}{\partial\theta\partial c} + \right. \\ & \left. \left( \frac{\partial\bar{c}}{\partial\xi} \right) \left( \frac{\partial\bar{\Omega}}{\partial\xi} \right) \frac{\partial^2 \mathfrak{R}}{\partial\Omega\partial c} + \left( \frac{\partial\bar{\theta}}{\partial\xi} \right) \left( \frac{\partial\bar{\Omega}}{\partial\xi} \right) \frac{\partial^2 \mathfrak{R}}{\partial\theta\partial\Omega} \right] \end{aligned} \quad (19a)$$

$$\begin{aligned} \frac{\partial\bar{\theta}}{\partial\tau} = & \frac{\partial^2 \bar{\theta}}{\partial\xi^2} - Z_e \mathfrak{R}(\bar{\theta}, \bar{\Omega}, \bar{c}) \\ & - \alpha Z_e \left[ \frac{1}{2} \left( \frac{\partial\bar{\theta}}{\partial\xi} \right)^2 \frac{\partial^2 \mathfrak{R}}{\partial\theta^2} + \left( \frac{\partial\bar{\theta}}{\partial\xi} \right) \left( \frac{\partial\bar{c}}{\partial\xi} \right) \frac{\partial^2 \mathfrak{R}}{\partial\theta\partial c} + \right. \\ & \left. \left( \frac{\partial\bar{c}}{\partial\xi} \right) \left( \frac{\partial\bar{\Omega}}{\partial\xi} \right) \frac{\partial^2 \mathfrak{R}}{\partial\Omega\partial c} + \left( \frac{\partial\bar{\theta}}{\partial\xi} \right) \left( \frac{\partial\bar{\Omega}}{\partial\xi} \right) \frac{\partial^2 \mathfrak{R}}{\partial\theta\partial\Omega} \right] \end{aligned} \quad (19b)$$

$$\frac{\partial}{\partial\xi} \left( (1 - S_{H_2O} \bar{c})^m \frac{\partial\bar{\Omega}}{\partial\xi} \right) = \pi \frac{\partial\bar{c}}{\partial\tau} \quad (19c)$$

where parameter  $\alpha$  is the correction parameter or coarse-grid parameter and is a function of coarse grid size.

The terms in square-brackets of Equations (19a) and (19b) are the corrections terms. However, the coarse-grid formulation is not closed and the correction parameter  $\alpha$  needs to be determined. It is expected that this parameter is a function of grid-size. In order to find the correction parameter  $\alpha$  a series of numerical experiments were conducted for different spatial grid sizes for each set of dimensionless groups (i.e.,  $Z_e$  and  $\pi$ ). The correction parameter  $\alpha$  for a specific reacting system can be determined by matching the coarse grid solution with the fine-grid or reference solution. To evaluate the improvement in accuracy, we define a numerical error as:

$$error = \left\{ \int (\psi - \bar{\psi})^2 d\xi \right\} / \left\{ \int \psi^2 d\xi \right\}^{1/2} \quad (20)$$

where  $\psi$  can be temperature, hydrate saturation or pressure.

The correction parameter is obtained by minimization of the numerical error given by equation (20). By repeating the matching process the correction parameter for different coarse-grid sizes can be obtained, and the coarse-grid formulation

(equations 19) is complete. This can then be used for subsequent large-scale simulation of hydrate decomposition. In the following, we use the above procedure for determining the parameter  $\alpha$ , and examine the success of this methodology in improving the accuracy of the coarse grid model.

## NUMERICAL RESULTS USING NEW FORMULATIONS

Equations 19 along with original boundary and initial equations (equations 10e to 10k) have been numerically solved using finite difference method in fully implicit scheme.

It was found that the terms involving the derivatives of dimensionless pressure in equation 19 may be ignored without loss of accuracy. The correction parameter  $\alpha$  is selected based on minimum error from the reference solutions. Figure 3 shows hydrate saturation, pressure and temperature profiles for reference solution (500) and for a coarse grid (100) solution with and without applying Taylor series correction for two different dimensionless times (20 right and 30 left). All the dimensionless groups and other properties are kept constant during this comparison ( $Ze = 1.69$  and  $\pi = 0.0025$ ). Figure 3 demonstrates the improvement in the coarse solution when the parameter  $\alpha$  equals 2.

Figure 4 shows the difference between the fine- and coarse-solutions (as expressed using equation 20) as a function of  $\alpha$ . It is observed that for different dimensionless times (20 right and 30 left) a constant value of  $\alpha$  gives the best results. This behavior was tested for other dimensionless times and a similar result was obtained. It was found that  $\alpha$  is independent of time and that a constant value of  $\alpha$  honors all relations given in Equation 21.

The same procedure was repeated for a different set of dimensionless parameters ( $Ze = 3.383$  and  $\pi = 0.00025$ ). Figure 5 shows that similar improvements were observed for  $\alpha$  equals 1.25 for two different dimensionless times (2 right and 3 left). Once again, regardless of the dimensionless time, a constant value of  $\alpha$  resulted in the most improvement (see Figure 6). To find a relation between the correction parameter and the grid size, a number of simulations were conducted, and results

were expressed using a dimensionless grid refinement ratio defined as the ratio of coarse grid block size to the fine grid block size  $\Delta\xi_{Coarse}/\Delta\xi_{fine}$ . The dimensionless groups were kept constant during these runs ( $Ze = 3.383$  and  $\pi = 0.00025$ ). The number of coarse grids were 50, 75, 100 and 125 while the reference or fine grid uses 500 grid blocks. For 50, 75, 100 and 125 coarse grid runs we were able to match the coarse grid using Taylor series improvement to the reference solution based on value of 6.1, 3.13, 2 and 1.35 for correction parameter respectively. Results in Figure 7 suggest that the relationship between correction parameter and dimensionless grid refinement may be approximated by a straight line. The generality of this observation requires further testing.

## DISCUSSION

In this work, a methodology for improvement of accuracy of coarse-grid simulation of hydrate decomposition by the depressurization method was presented. However, this work has a number of limitations that are the subject of our current research. These include:

- The correction parameter needs to be determined as a function of dimensionless groups identified in this work ( $Ze$  and  $\pi$ )
- The applicability of this methodology needs to be demonstrated in numerical simulators that do not include the assumptions made in this study.
- The applicability of this method needs to be tested for 2D and 3D problems, where a major enhancement in computation time may be achieved.

Despite these limitations, the major contributions of this work include:

- Demonstrating that the coarse-grid formulation may be modified to improve accuracy.
- Once a correction parameter  $\alpha$  is obtained, the correction terms, are a function of the coarse-grid solution alone (see Equation 19).
- It was found that a single correction parameter  $\alpha$  is sufficient to improve the accuracy of all coarse-grid variables (pressure, temperature and hydrate saturation). However, the correction parameter is a function of grid-block size and dimensionless groups controlling the solution.

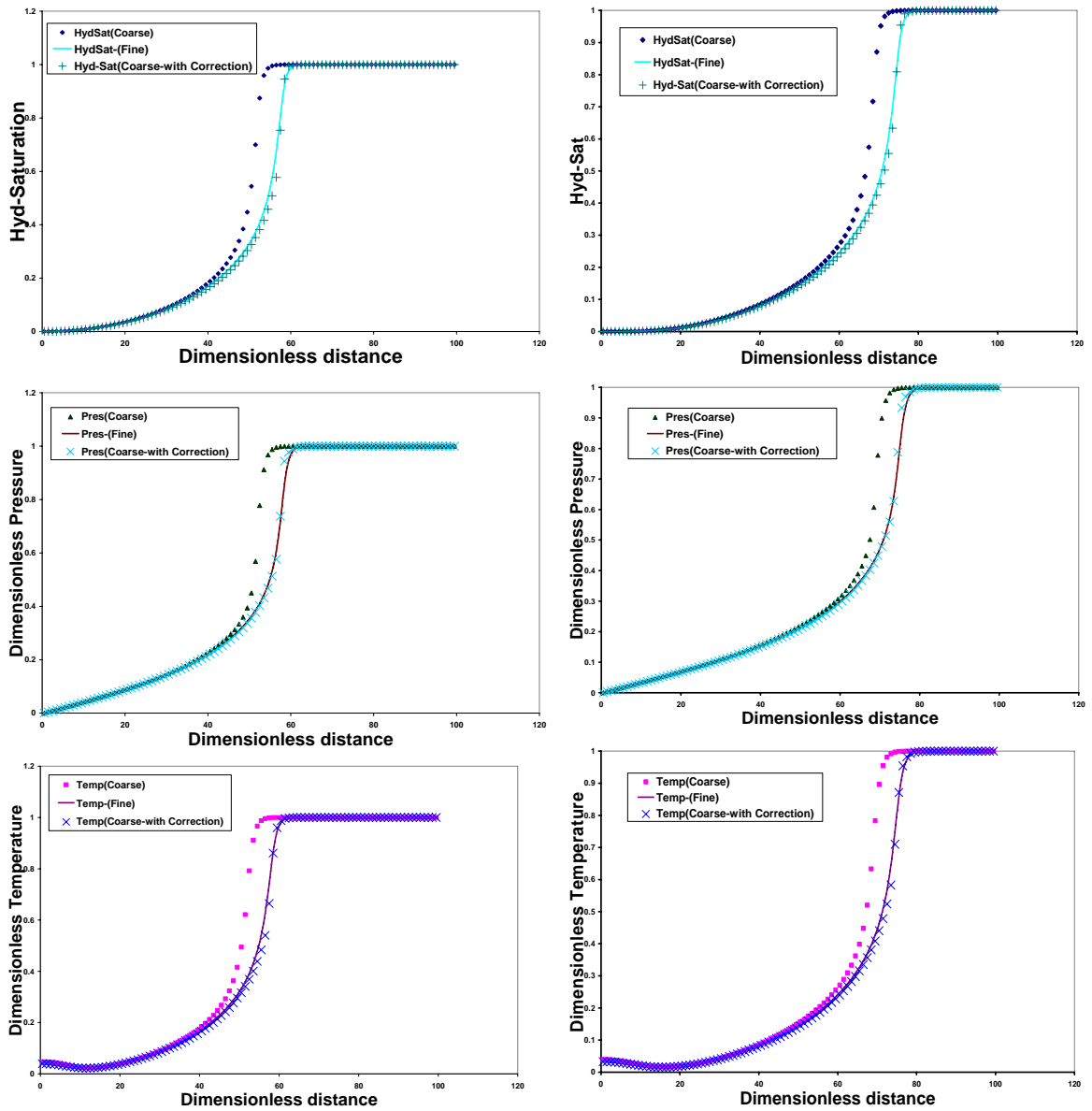


**Figure 3:** Dimensionless hydrate saturation, pressure and temperature for fine and coarse grid with and without correction at dimensionless time = 20 (left) and 30 (right),  $Ze = 1.69$  and  $\pi = 0.0025$ .

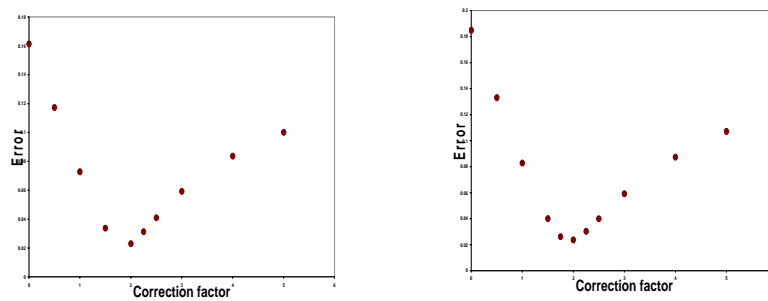


**Figure 4:** Error (from the reference solution) as a function of correction parameter for at dimensionless time = 20 (left) and 30 (right),  $Ze = 1.69$  and  $\pi = 0.0025$ .

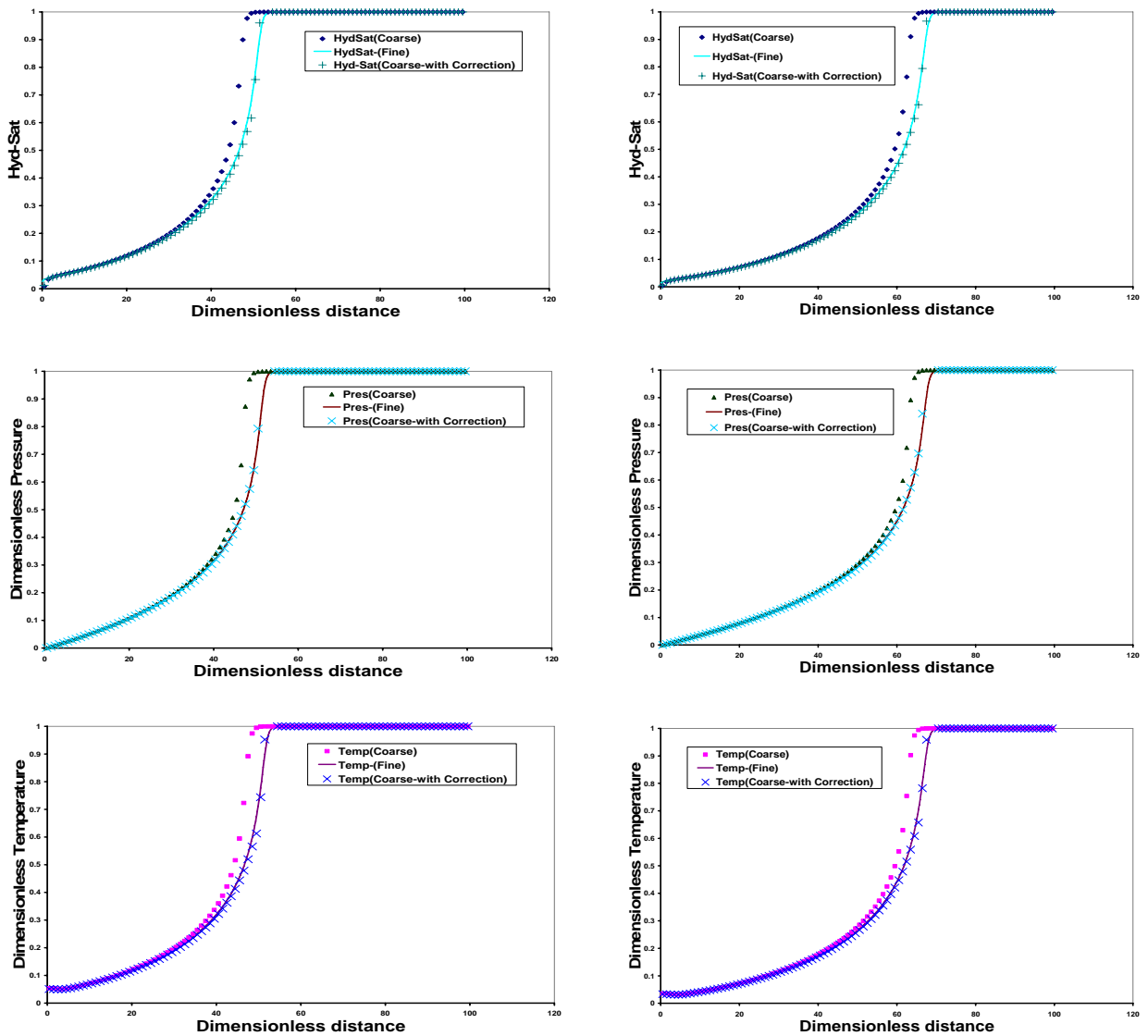


**Figure 5:** Dimensionless hydrate saturation, pressure and temperature for fine and coarse grid with and without correction at dimensionless time = 2 (left) and 3 (right)  $Ze = 3.383$  and  $\pi = 0.00025$ .

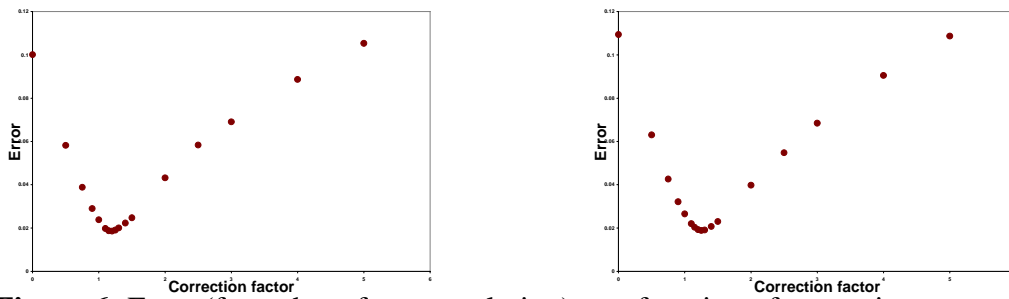


**Figure 6:** Error (from the reference solution) as a function of correction parameter for dimensionless time = 2 (left) and 3 (right),  $Ze = 3.383$  and  $\pi = 0.00025$ .

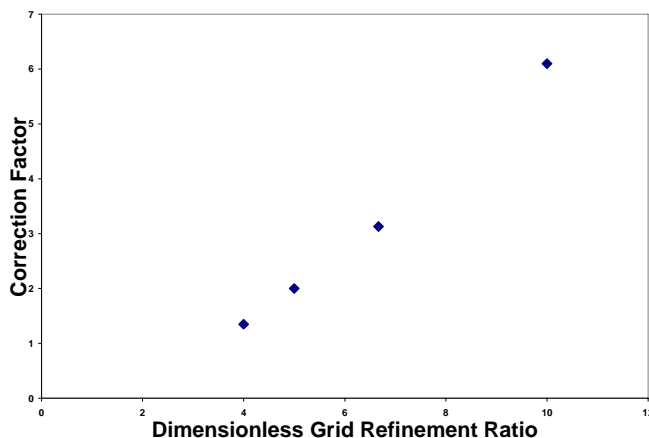


**Figure 7:** Correction parameter as a function of grid-ratio  $Ze = 1.69$  and  $\pi = 0.0025$

## SUMMARY AND CONCLUSIONS

Depending on how pressure reduction can diffuse within the hydrate layer, a narrow decomposition zone can exist during gas production from hydrate reservoirs. A large contrast in the length scale of the decomposition zone and that of diffusive heat and mass transfer makes the process difficult to resolve numerically unless a large number of numerical grid cells are used. Such numerical simulations are computationally expensive to perform.

In this study, a coarse-grid formulation for numerical modeling of a one-dimensional gas hydrate decomposition system is presented. The presented formulation is based on a Taylor series expansion of the reaction term and presents the modification of the reaction term in the coarse model that would allow an accurate solution. A key parameter in this formulation is  $\alpha$  or coarse-grid correction parameter, which is a function of the coarse-grid size. The value of  $\alpha$  for each coarse-grid model and each set of dimensionless groups can be obtained by minimizing the deviation errors of coarse-grid simulations from fine or reference solutions. This parameter then can be used for numerically solving a large scale and computationally intensive case. It is shown that by considerably reducing the numerical error, this formulation could match the fine grid numerical solution. In addition, for the cases tested it was found that the coarse-grid correction parameter  $\alpha$  has a linear relationship with dimensionless grid

refinement number defined as the ratio of coarse grid block size to the fine grid block size. Results obtained in this study for a one-dimensional problem are promising in terms of reducing computational time. We anticipate that the computational time saving for multi-dimensional problems is more promising. The presented formulation improves our capabilities for conducting more accurate and faster numerical simulation of industrial scale gas hydrate reservoirs.

## ACKNOWLEDGMENT

This work was supported through grants from the Computer Modeling Group (CMG) and the CTTII program of the Natural Resources Canada (NRCan)

## REFERENCES

1. SELIM, M.S. and SLOAN, E.D.: "Modeling of the Dissociation of an In-situ Hydrate," paper SPE 13597 presented at the 1985 SPE California Regional Meeting, Bakersfield, March 27-29
2. SELIM, M.S. and SLOAN, E.D., Hydrate Dissociation in Sediment; *SPE Reservoir Engineering*, Vol. 5, No. 2, pp. 245-251, May 1990
3. TSYPKIN, G.G., Mathematical Models of Gas Hydrates Dissociation in Porous Media; *Gas Hydrates: Challenges for the Future*, edited by Holder G.D. and Bishnoi P.R., Vol. 912, pp. 428-436, New York: New York Academy of Sciences, 2000.
4. HONG, H., POOLADI-DARVISH, M., and BISHNOI, P.R., Analytical Modeling of Gas Production from Hydrates in Porous Media; *paper 2002-113, JCPT*.

5. Shahab Gerami, Mehran Pooladi-Darvish. "Predicting gas generation by depressurization of gas hydrates where the sharp-interface assumption is not valid" *Journal of Petroleum Science and Engineering* 56 (2007) 146-164.
6. Shahab Gerami, Mehran Pooladi-Darvish, "Material Balance and Boundary Dominated Flow Models for Hydrate-Capped Gas Reservoirs". SPE paper 102234, *presented at the 2006 SPE Annual Technical Conference and Exhibition held in San Antonio, Texas, USA. 24-27 September 2006.*
7. HOLDER, G.D. and ANGERT, P.F., Simulation of Gas Production From a Reservoir Containing Both Gas Hydrates and Free Natural Gas; *paper SPE 11105, presented at the 1982 SPE Annual Technical Conference and Exhibition, New Orleans, LA, September 26 – 29, 1982*
8. BURSHEARS, M., O'BRIEN, T.J., and MALONE, R.D., A Multi-Phase, Multi-Dimensional, Variable Composition Simulation of Gas Production From a Conventional Gas Reservoir in Contact With Hydrates; *paper SPE 15246, presented at the 1986 SPE Unconventional Gas Technology Symposium, Louisville, KY, May 18– 21, 1986.*
9. YOUSIF, M.H., ABASS, H.H., and SLOAN, E.D., Experimental and Theoretical Investigation of Methane-Gas-Hydrate Dissociation in Porous Media; *SPE Reservoir Engineering, Vol. 6, No. 1, pp. 69-76, February 1991.*
10. MORIDIS, G.J., Numerical Studies of Gas Production From Methane Hydrates; *paper SPE 75691, presented at the SPE Gas Technology Symposium, Calgary, AB, April 30 – May 2, 2002.*
11. Hong, H. and Pooladi-Darvish, M.: "A Numerical Study on Gas Production from Formations Containing Gas Hydrates," paper CIPC 2003-60 presented at the 2003 CIPC Conference, Calgary, AB, June 10–12.
12. George J. Moridis, Michael B. Kowalsky and Karsten Pruess, "Depressurization-Induced Gas Production From Class 1 Hydrate Deposits" *paper SPE 97266 presented at the 2005 SPE Annual Technical Conference and Exhibition held in Dallas, Texas, USA., 9-12 October 2005.*
13. Sun, X., Mohanty, K.K., "Kinetic simulation of methane hydrate formation and dissociation in porous media" *Chemical Engineering Science* 61 (2006) 3476 – 3495.
14. Zatsepina, O., Hong, H., and Pooladi-Darvish, M.: "Behavior of Gas Production from Type III Hydrate Reservoirs," presented at the paper presented at the 6<sup>th</sup> International Conference on Gas Hydrates, July 6-10, 2008, Vancouver, BC.
15. KIM, H.C., BISHNOI, P.R., HEIDEMANN, R.A., and RIZVI, S.S.H., Kinetics of Methane Hydrate Decomposition; *Chemical Engineering Science, Vol. 42, No. 7, pp. 1645-1653, 1987.*
16. Sloan, E.D., "Clathrate Hydrates of Natural Gases", 2nd edition., Marcel Dekker, New York (1998).
17. Masuda, Y., Naganawa, S., Ando, S., and Salo, K., "Numerical Calculation of Gas-Production Performance from Reservoir Containing Natural Gas Hydrate", SPE38291, Society of Petroleum Engineers(1997).
18. HONG, H., Modelling of Gas Production From Hydrates in Porous Media; *M.Sc. Thesis, University of Calgary, 2003.*
19. Daniel A. Schult, Matched asymptotic expansions and the closure problem for combustion waves, *SIAM J. Appl. Math.*, 60 (1999), pp. 136-155.
20. Dmitry Golovaty: On Step-Function Reaction Kinetics Model in the Absence of Material Diffusion. *SIAM Journal of Applied Mathematics* 67(3): 792-809 (2007)
21. C. Meile, K. Tuncay, Scale dependence of reaction rates in porous media, *Adv. Water Resour.* 29 (2006) 62-71.
22. B.D. Wood, S. Whitaker, Diffusion and reaction in biofilms, *Chem. Eng. Sci.* 53 (1998) 397–425. Erratum to diffusion and reaction in biofilms. *Chem. Eng. Sci.* 55 (2000) 2349.
23. B.D. Wood, S. Whitaker, Multi-species diffusion and reaction in biofilms and cellular media. *Chem. Eng. Sci.* 55 (2000) 3397-3418.
24. B. D. Wood, K. Radakovich, F. Golfier, Effective reaction at a fluid–solid interface: Applications to biotransformation in porous media, *Adv. Water Resour.* 30 (6-7) (2006) 1630-1647.
25. B.D. Wood, F. Cherblanc, M. Quintard, S. Whitaker, Volume averaging for determining the effective dispersion tensor: Closure using periodic unit cells and comparison with ensemble averaging, *Water Resour. Res.* 39(8) (2003) 1210.